

**Self-assembling nano mixed-brushes having co-continuous surface morphology by melt growing single crystals and comparison with solution patterned leopard-skin surface morphology**

S. Agbolaghi<sup>a,b</sup>, M. Alizadeh-Osgouei<sup>a,b</sup>, S. Abbaspoor<sup>a,b</sup>, F. Abbasi<sup>a,b,\*</sup>

<sup>a</sup> Institute of Polymeric Materials, Sahand University of Technology, Tabriz, Iran

<sup>b</sup> Faculty of Polymer Engineering, Sahand University of Technology, Tabriz, Iran

**Experimental**

**Materials**

Polyethylene glycol monomethyl ether 5000 (PEG) (Aldrich) was dried before use by removing residual water by azeotropic distillation with toluene (Merck, > 99%) on a water separator. 4-(Dimethylamino) pyridine (DMAP, Merck) and 2,2'-bipyridine(bipy, Merck, 98%) were used as received without purification. Methylene dichloride ( $\text{CH}_2\text{Cl}_2$ , Merck, > 99.5%) was shaken with concentrated  $\text{H}_2\text{SO}_4$  (Merck, 95-97%) until the acid layer remained colorless, then washed with water, and finally distilled with  $\text{CaH}_2$  (Merck, ~ 95%). 2-Bromoisobutyryl bromide (Merck) was distilled under vacuum. Triethylamine (TEA, Merck, > 99%) was stored with  $\text{CaH}_2$  over night, and then distilled. Inhibitors in styrene (St, Merck, > 99%) and methyl methacrylate (MMA, Merck, > 99%) were removed by passing the monomers over an alumina column, and then

---

\* Corresponding author

E-mail address: f.abbasi@sut.ac.ir

distilled under reduced pressure. CuBr (Alfa Aesar, 98%) and CuCl (Merck,  $\geq$  97%) were purified by stirring with glacial acetic acid (Merck, > 99.8%), filtered and washed three times with ethanol (Merck, 99.5%) and twice with diethyl ether (Merck, > 99%), and finally dried under vacuum. Chlorobenzene (CB, Merck, > 99%) was washed with concentrated H<sub>2</sub>SO<sub>4</sub> to remove thiophenes, and then distilled over anhydrous calcium chloride (Merck). All other reagents were purchased from commercial sources and used as received without purification.

## Methods

The bromo-capped (PEG) macroinitiator (PEG-Br) was synthesized according to the literature [1]. In an experiment a 7.50 mmol DMAP in 10 mL dried methylene dichloride was mixed with 5.00 mmol TEA. The solution was transferred into a 250 mL three-neck round-bottom flask equipped with a reflux condenser, dropping funnel, gas inlet/outlet, and a magnetic stirrer. After cooling to 0 °C, a solution of 12.50 mmol 2-bromoisobutyryl bromide in 10 mL CH<sub>2</sub>Cl<sub>2</sub> was added under stirring. Then a solution of 5 mmol PEO in 50 mL dried CH<sub>2</sub>Cl<sub>2</sub> was added dropwise into flask slowly in 1 h, and a yellow dispersion was formed. Subsequently, the temperature was increased to room temperature. The reaction was let proceed under stirring for 18 h. Finally, the crude product was filtered, precipitated with cold diethyl ether, recrystallized from ethanol, washed with cold diethyl ether and dried under vacuum at room temperature [1,2]. The diblock copolymers of PEG-*b*-PS and PEG-*b*-PMMA including various molecular weights of PS and PMMA blocks were synthesized via solution polymerization in chlorobenzene by normal atom transfer radical polymerization (ATRP).

In a typical batch, a glass reactor with two vacuum valves, in order to purge with pure nitrogen, and an inlet in its uppermost part to charge and discharge the materials, was filled with appropriate ratio of monomer, PEG-Br macroinitiator, catalyst ( $\text{CuBr}$  and  $\text{CuCl}$  for St and MMA polymerization, respectively), bipy as a ligand and chlorobenzene as solvent ( $([\text{St}]_0/[\text{MI}]_0/[\text{CuBr}]_0/[\text{bipy}]_0/[\text{CB}]_0)=240/1/1/3/66$ ) and ( $([\text{MMA}]_0/[\text{MI}]_0/[\text{CuCl}]_0/[\text{CuCl}_2]_0/[\text{bipy}]_0/[\text{CB}]_0)=177/1/1/0.07/3/375$ ). After purging with high purity nitrogen, for 20 minutes, the valves and inlet were closed, and the reactor was immersed in a thermostatic oil bath at desired temperature (110 and 65°C for St and MMA polymerization, respectively). Due to higher reactivity of MMA in comparison with St [3,4],  $\text{CuCl}_2$  was used as deactivator for better controlling of polymerization [5]. The system was usually stirred to ensure better contact of reagents. After passing desired time, the reactor was cooled to room temperature. The reaction mixture was diluted with tetrahydrofuran (THF, Merck, > 99.5%) and then was filtered through a neutral  $\text{Al}_2\text{O}_3$  (Merck, 70-230 mesh ASTM) column to remove the catalyst, and precipitated with petroleum ether (Merck, >95%). The synthesized diblock copolymers were obtained and dried under vacuum overnight at room temperature. (Characteristic of ATRP, the GPC traces (Figure S1) are narrow, symmetric, mono-modal, and move with increasing conversion towards lower elution volume, i.e. elevated molecular weights. The molecular characterization data of diblock copolymers used in this work are reported in Table S1. Thermal data points were gathered by differential scanning calorimetry (DSC) (Netzsch, F3 Maia) and the polydispersities were determined by GPC on a Water 1515 gel permeation chromatography instrument with a set of HT3, HT4, and HT5,  $\mu$ -styrigel columns with DMF as an eluent (1.0 mL/min) at 35 °C.

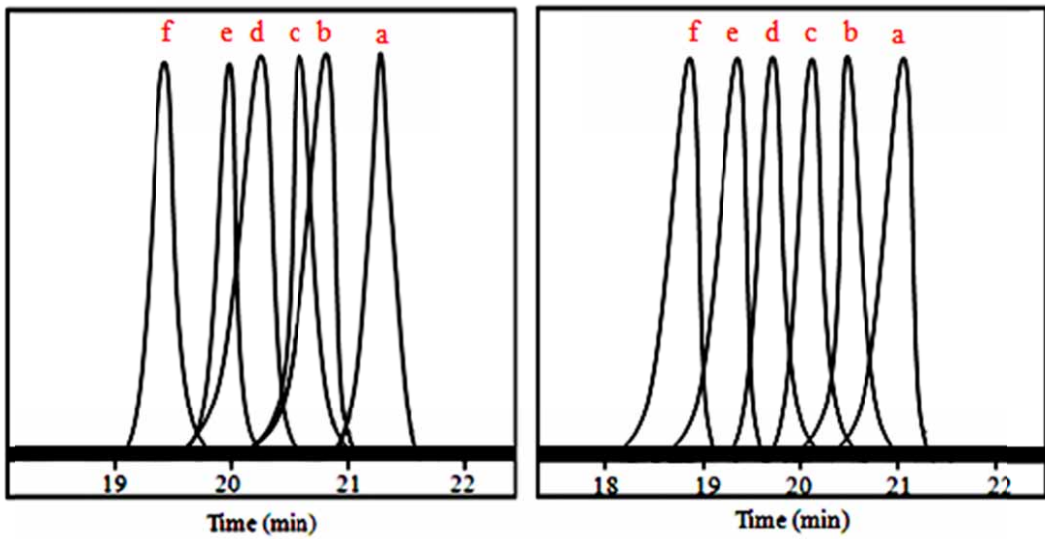


**Fig. S1.** Evolution of GPC traces with polymerization time. (Left) PEG<sub>5000</sub>-*b*-PS<sub>4600</sub> (a), PEG<sub>5000</sub>-*b*-PS<sub>7800</sub> (b), PEG<sub>5000</sub>-*b*-PS<sub>10000</sub> (c), PEG<sub>5000</sub>-*b*-PS<sub>12500</sub> (d), PEG<sub>5000</sub>-*b*-PS<sub>14800</sub> (e) and PEG<sub>5000</sub>-*b*-PS<sub>18500</sub> (f); (Right) PEG<sub>5000</sub>-*b*-PMMA<sub>8700</sub> (a), PEG<sub>5000</sub>-*b*-PMMA<sub>11000</sub> (b), PEG<sub>5000</sub>-*b*-PMMA<sub>13100</sub> (c), PEG<sub>5000</sub>-*b*-PMMA<sub>15200</sub> (d), PEG<sub>5000</sub>-*b*-PMMA<sub>17100</sub> (e), and PEG<sub>5000</sub>-*b*-PMMA<sub>19300</sub> (f).

**Table S1.** Characteristics of PEG-*b*-PS and PEG-*b*-PMMA diblock copolymers and relative single crystals

Sample	T <sub>m</sub> of diblock copolymers (°C)	T <sub>m</sub> of single crystal mat (°C)	T <sub>g</sub> (°C)	PDI
PEG <sub>5000</sub> - <i>b</i> -PS <sub>4600</sub>	59.51	63.71	63.30	1.08
PEG <sub>5000</sub> - <i>b</i> -PS <sub>7800</sub>	57.10	61.21	69.45	1.08
PEG <sub>5000</sub> - <i>b</i> -PS <sub>10000</sub>	55.92	59.87	74.70	1.06

---

PEG <sub>5000</sub> - <i>b</i> -PS <sub>12500</sub>	54.01	58.11	79.12	1.09
PEG <sub>5000</sub> - <i>b</i> -PS <sub>14800</sub>	52.54	56.13	82.20	1.07
PEG <sub>5000</sub> - <i>b</i> -PS <sub>18500</sub>	49.68	53.83	88.13	1.08
PEG <sub>5000</sub> - <i>b</i> -PMMA <sub>8700</sub>	56.72	60.42	86.78	1.12
PEG <sub>5000</sub> - <i>b</i> -PMMA <sub>11000</sub>	55.35	59.03	89.90	1.13
PEG <sub>5000</sub> - <i>b</i> -PMMA <sub>13100</sub>	53.30	56.94	92.46	1.12
PEG <sub>5000</sub> - <i>b</i> -PMMA <sub>15200</sub>	51.50	55.25	94.97	1.13
PEG <sub>5000</sub> - <i>b</i> -PMMA <sub>17100</sub>	50.41	54.01	97.02	1.11
PEG <sub>5000</sub> - <i>b</i> -PMMA <sub>19300</sub>	48.01	52.41	99.81	1.12

---

### Single crystal growth limitations in melt state

When the bulk of crystallizable chains on the silicon wafer is not enough after passing a given time, a discretizing will be happened on the silicon wafer surface. In better words, when single crystals begin to grow from left seeds from self-seeding, only a limit assortment of chains could diffuse and drop off to the developing single crystal. Eventually, when the given time passed, a loop of depletion region will surround the area of chain supplier. The images of AFM and optical microscope proved this phenomenon. So, the content of chains dispersed homogeneously on the silicon wafer is very important. The concentration of polymer chains is homogeneous on all over the silicon surface; but in the secondary crystallization level, only the chains could adhere to the

seeds that have presence in this critical area. Hence, depending on the primary concentration of diblock chains, the longer time in secondary crystallization level would not lead to greater lateral size. Quantitatively explain, for PEG<sub>5000</sub>-*b*-PMMA<sub>17100</sub>/PEG<sub>5000</sub>-*b*-PS<sub>10000</sub> mixed-brush single crystal at T<sub>c</sub>= 23 °C, after passing 60 and 72 h the lateral sizes were 23.11 and 23.13 μm, respectively.

Another restriction in melt growth systems is that when the concentration of polymer chains is too high (to reach to higher lateral sizes), the population of non-ideal structures will increase. Exemplarily, by changing the amount of diblock copolymers from 10 to 20 mg on a given surface area of silicon wafer, the population of ideal single crystals decreased significantly. So, the amount of polymer chains should be optimized to reach to maximum population of ideal single crystals together with the largest lateral size, simultaneously.

### **Higher regimes in melt state**

In this work, totally, the brushes fabricated from melt-grown single crystals are embedded in higher regimes than those in solution-grown mixed-brush single crystals [1]. In details, for PMMA brushes, the growth condition has changed from poor (amyl acetate at T<sub>c</sub>= 23-30 °C [2]) to theta condition [3,4] (melt of block copolymer chains). Besides, the crystalline substrates thicknesses of PMMA-covered phase regions in melt state are considerably higher than those in solution state. As an instance for PMMA<sub>8700</sub>-covered substrates in melt and solution at T<sub>c</sub>= 23 °C, the thicknesses are equal to 7.77 and 3.50 nm, respectively. On the other hand, for PS-covered phase regions, we cannot judge only on the basis of substrate thicknesses; because the condition has altered from very good (amyl acetate at T<sub>c</sub>= 23-30 °C) [5] to theta [3,4], and this can in turn lead to higher thicknesses. Therefore, we intend to compare the reduced tethering

densities ( $\tilde{\sigma}$ ) [5,6,7] in growth systems. For example at  $T_c = 23$  °C for PS<sub>10000</sub>-covered phase regions,  $\tilde{\sigma}$  was 24.96 and 21.48 for melt and solution systems. Another instance reports the values of  $\tilde{\sigma}$  in PS<sub>14800</sub>-covered areas at  $T_c = 30$  °C. Here,  $\tilde{\sigma}$  is 42.10 and 30.21 for melt and solution-grown single crystals.

### The exclusive effect of amorphous brushes molecular weight

Previously in solution growth systems, the features of each phase region affected only its own thickness. Simply, keeping all other effective parameters at a certain point and varying  $M_n^{\text{PMMA}}$  as a type, only the overall thickness of PMMA-covered phase regions underwent related changes. For example the total, substrate and amorphous brushes thickness for  $M_n^{\text{PMMA}} = 8700$  g/mol at  $T_c = 30$  °C in all samples were somehow 25.5, 9 and 8.2 nm, respectively. Mentioned relation satisfied the condition of PS systems as well. Likewise, now in melt-grown mixed-brush single crystals this phenomenon was also pleased. As an instance the total, substrate and amorphous brushes thickness for  $M_n^{\text{PS}} = 14800$  g/mol at  $T_c = 23$  °C in all samples were to an extent 38, 8.5 and 14.8 nm, respectively.

### References

1. Abbaspoor, S; Abbasi, F; Agbolaghi, S. RSC Advances 2014, 4,17071.
2. Brandup, J.; Immergut, E. H. Polymer Handbook; Wiley: New York, 1975.
3. Rubinstein, M.; Polymer physics; Oxford University Press, 2003.
4. Sperling, L. H.; Introduction to physical polymer science, John Wiley, 2006.
5. Zheng, J. X.; Xiong, H.; Chen, W.Y.; Lee K.; Van Horn, R. M.; Quirk, R. P.; Lotz, B.; Thomas, E. L.; Shi, A. -C.; Cheng, S. Z. D. *Macromolecules* 2006, 39, 641.

6. Fetters, L. J.; Hadjichristidis, N.; Lindner, J. S.; Mays, J. W. *J. Phys. Chem.* 1994, 23, 619.
7. Kent, M. S. *Macromol. Rapid Commun.* 2000, 21, 243.